

Minerva Access is the Institutional Repository of The University of Melbourne

Author/s:

Ermine, CM;Nithianantharajah, J;O'Brien, K;Kauhausen, J;Frausin, S;Oman, A;Parsons, MW;Brait, VH;Brodtmann, A;Thompson, LH

Title:

Hemispheric cortical atrophy and chronic microglial activation following mild focal ischemic stroke in adult male rats

Date:

2021-12-01

Citation:

Ermine, C. M., Nithianantharajah, J., O'Brien, K., Kauhausen, J., Frausin, S., Oman, A., Parsons, M. W., Brait, V. H., Brodtmann, A. & Thompson, L. H. (2021). Hemispheric cortical atrophy and chronic microglial activation following mild focal ischemic stroke in adult male rats. *Journal of Neuroscience Research*, 99 (12), pp.3222-3237. <https://doi.org/10.1002/jnr.24939>.

Persistent Link:

<https://hdl.handle.net/11343/299092>

DR STEFANO FRAUSIN (Orcid ID : 0000-0001-8536-5241)

Article type : Research Article

Hemispheric cortical atrophy and chronic microglial activation following mild focal ischemic stroke in adult male rats.

Long-term impacts of mild stroke.

Charlotte M. Ermine, PhD*¹, Jess Nithianantharajah, PhD¹, Katrina O'Brien, BSc¹, Jessica A Kauhausen PhD¹, Stefano Frausin PhD¹, Alexander Oman, MSc¹, Mark W. Parsons MD, PhD^{2,5}, Vanessa H. Brait, PhD¹, Amy Brodtmann#, MD, PhD^{1,3,4} and Lachlan H. Thompson#, PhD¹

¹ The Florey Institute of Neuroscience and Mental Health, University of Melbourne, Melbourne, Australia

² Melbourne Brain Centre, University of Melbourne, Melbourne, Australia.

³ Department of Neurology, Austin Health, Melbourne, Australia

⁴ Eastern Cognitive Disorders Clinic, Eastern Health, Monash University, Australia.

⁵ University of New Wales South Western Clinical School, Ingham Institute for Applied Medical Research, and Department of Neurology, Liverpool, Australia.

*Corresponding author: charlotte.ermine@florey.edu.au

#These authors contributed equally to this work.

This is the author manuscript accepted for publication and has undergone full peer review but has not been through the copyediting, typesetting, pagination and proofreading process, which may lead to differences between this version and the [Version of Record](#). Please cite this article as [doi: 10.1002/JNR.24939](https://doi.org/10.1002/JNR.24939)

This article is protected by copyright. All rights reserved

Keywords: Brain infarction, Endothelin-1, neurodegeneration, stroke, microglia, touchscreen, RRID:AB_10711153, RRID:AB_2811075, RRID:AB_566455, RRID:SCR_017654, RRID:SCR_002798.

Funding: This work was supported by an NHMRC project grant #1094974 and an NHMRC Disease Teams Research Grant. CE was supported by NHMRC Program Grant #1113352 ‘Saving Brain and Changing Practice in Stroke’. JN was supported by the Australian Research Council Future Fellowship #140101327.

Conflict of interest: The authors declare no conflict of interest.

Compliance with Ethical Standards: The experimental design and procedures were approved by the Florey Institute for Neuroscience and Mental Health Animal Ethics Committee. All applicable international, national, and/or institutional guidelines for the care and use of animals were followed.

Significance Statement

Animal modelling of stroke has overwhelmingly focused on severe forms, with analysis limited to the sub-acute phase. However, stroke severity is highly heterogenous and there is increasing evidence suggesting that moderate infarcts, including subclinical stroke, lead to cognitive decline in the chronic phase. Thus, we describe a mild cortical infarction in rats that model features of subclinical human stroke. The results show multiple levels of long-term impact, including cortical atrophy, increased hippocampal neurogenesis and increased inflammation persisting up to one year. These outcomes highlight that atrophy and inflammation are interesting targets for therapeutic intervention in chronic phase after mild stroke.

Abstract

Animal modelling has played an important role in our understanding of the pathobiology of stroke. The vast majority of this research has focussed on the acute phase following severe forms of stroke that result in clear behavioural deficits. Human stroke, however, can vary widely in severity and clinical outcome. There is a rapidly building body of work suggesting that milder ischaemic insults can precipitate functional impairment, including cognitive decline, that continues through the chronic phase after injury. Here we show that a small infarction localised to the frontal motor cortex of rats following injection of endothelin-1 (ET-1) results in an essentially asymptomatic state based on motor and cognitive testing, and yet produces significant histopathological change including remote atrophy and inflammation that persists up to 1 year. While there is understandably a major focus in stroke research on mitigating the acute consequences of primary infarction, these results point to progressive atrophy and chronic inflammation as additional targets for intervention in the chronic phase after injury. The present rodent model provides an important platform for further work in this area.

Introduction

The majority of pre-clinical stroke research deals with moderate to severe strokes and analysis of acutely definable anatomical and behavioural outcomes over days or weeks [1], [2]. Human strokes, however, can be milder in severity when they involve smaller vessels or only involve brief periods of ischaemia, and can manifest as silent brain infarcts, microinfarcts or transient ischemic attacks (TIA). These strokes are often asymptomatic, or present with transient symptoms that resolve within hours of the event. Silent brain infarction, also called subclinical stroke, is common. In the Northern Manhattan Study (NOMAS), almost 18% of participants in their multiethnic community-based cohort were found to have silent brain infarcts [3]. Importantly, one of the biggest drivers of cognitive decline is silent brain infarction [4], [5]. Dhamoon *et al* (2019) reported that silent brain infarction detected on serial MRI scanning was associated with a 3-fold greater cognitive decline among those with silent infarction than in those without. In a 2019 meta-analysis, Lei *et al* (2019) concluded that rather than being clinically silent, silent brain infarction may be a major factor in the induction of cognitive impairment and decline [4]. Thus, understanding the long-term effects of ‘minor’ stroke is extremely important, as mild ischemic events are

more prevalent than currently recognised [6]. Their incidence is likely underestimated as they are often asymptomatic or present transient symptoms, for which the person is unlikely to seek medical attention. Post-mortem studies have shown the presence of microinfarcts in the brain of 33% of cognitively healthy adults [7].

While many advances in understanding stroke pathology have been made in recent years, the relationship between mild ischemic injury and cognitive decline later in life is poorly understood. One possibility is the chronic activation of inflammatory cascades that induce secondary neuronal damage, axonal degeneration and brain atrophy. There are currently few animal studies that have modelled and examined the pathophysiology of mild ischemic injury and the majority of these limit their analyses to the acute or subacute phase of the injury over days or weeks [8], [9]. A single study in marmosets showed the accumulation of TDP43 and APP over 12 months [10] but there are currently no studies of mild stroke spanning longer than this timeframe in rodents.

Isolated cortical lesions are a common imaging finding in the 30% of patients presenting with transient ischemic attacks who are then found to have infarcts on imaging. Importantly, isolated cortical infarcts are highly represented in silent brain infarction: the exact model we were trying to replicate in this study. Up to 80% of silent brain infarcts have been demonstrated to be cortically located, especially in post-surgical, high vascular risk populations [11]. Microinjection of the potent vasoconstrictor endothelin-1 has become a widely used approach to model focal ischemic injury in rodents with the capacity to modulate severity based on dosage [12]. We recently reported that ET-1 injection into the sensorimotor cortex of athymic rats that have a compromised immune system, resulted in a focal ischemic injury associated with a stable motor impairment over 36 weeks [13]. It prompted us to explore motor and cognitive impacts in the present study using Long-Evans, an outbred strain most commonly employed in rat behavioural studies. Interestingly, we found that the Long-Evans strain is markedly less sensitive to ET-1-induced infarction such that the same dose and injection parameters produced a mild ischemic injury that did not result in any detectable motor dysfunction or cognitive impairment in attentional processing using a touchscreen-based continuous performance task over 12 months. This provided a unique opportunity to assess long-term pathological changes in a rodent model of mild ischemia analogous to human asymptomatic, silent brain infarcts. The results showed multiple levels of long-term impact following mild ischemic injury, including hemispheric cortical atrophy, increased hippocampal neurogenesis and an increased level of inflammation in multiple nuclei persisting for up to one year.

Materials and Methods

Surgical procedures and study design

A total of 95 adult (22 weeks), male Long Evans rats were used in this study. The experimental design and procedures were approved by the Florey Institute for Neuroscience and Mental Health Animal Ethics Committee. All animals were housed in pairs under a 12h light/dark cycle with *ad libitum* access to food and water. This work followed the recommendations of the Stroke Therapy Academic Industry Roundtable (STAIR).

Animals under deep anaesthesia (2% isoflurane) were placed in a stereotaxic frame and focal ischemic injury was induced by injection of the vasoconstrictor, ET-1 (800pmol in saline; AusPep), into the sensorimotor cortex at two sites (0.5 and 2.0 mm rostral and 2.8 mm lateral to bregma and 1.5 mm below the surface of the brain) as previously described [13]. Control animals received the same volume of saline injected at the same co-ordinates.

A first cohort of animals were used for histological analysis at 1, 4, 12, 24, 36 and 48 weeks post-surgery (n=6 allocated per group for each time-point, based on our previous work using this model [13]). Two rats died during the surgical procedure and two others spontaneously developed tumour growth during the course of the experiment leading to immediate euthanasia. The final group numbers for histological analysis were: 1week - ET-1 and Saline (n=5); 4 weeks - ET-1 (n=6), Saline (n=5); 24 weeks - ET-1(n=5), Saline (n=6); 12, 36 and 48 weeks - ET-1 and Saline (n=6). A second cohort underwent touchscreen training for 8 weeks prior to surgery followed by longitudinal touchscreen testing at 1, 4, 12, 24, 36 and 48 weeks, and staircase testing at 4 weeks (ET-1, n=13; Saline, n=9, based on our previous work using this model [13]). In this group one rat died during surgery and one was euthanised as a result of tumour growth, bringing the final behavioural group numbers to: Saline - Pre-Stroke to 36 weeks, (n=10); 48 weeks (n=9) and ET-1 - Pre-Stroke to 12 weeks (n=13); 24 to 48 weeks (n=12).

BrdU treatment

We were interested to see if this was accompanied by chronic changes in hippocampal neurogenesis. Animals were injected with the thymidine analogue 5-bromo-2'-deoxyuridine

(BrdU) with 100mg/kg doses at 12h intervals over 3 days beginning 4 weeks prior to the 12, 24, 36 and 48 week time-points for histological analysis.

Staircase testing

The staircase test was used to test motor performance as previously described [14], [15]. Briefly, the animals were placed in a staircase apparatus (Campden Instruments, United Kingdom) in a dark room for 20 minutes, where each forelimb had access to 50 sugar pellets positioned on steps 2-6. The total number of pellets eaten using each forelimb was recorded daily for each session over two weeks and expressed as the average performance of the last 3 days. Pretraining was done over 2 weeks before the stroke and testing was done 4 weeks post-stroke. Animals who did not retrieve at least 20 pellets using their unimpaired limb were excluded from the analysis. The test was performed blinded to saline (n=9) and ET-1 (n=13).

Attention testing in the rodent touchscreen system

Rats were housed in pairs in open-top cages under reverse light cycle (12h:12h, lights off at 0700 hours). Behavioural testing was conducted during the dark (active) phase of the cycle. Rats were handled and began training in the touchscreen chambers at 8 weeks of age. Rats were food restricted to ~85-90% free-feeding body weight only during touchscreen testing. Prior to surgery and at all other times between behavioural testing, rats received *ad libitum* access to food. Water was available *ad libitum* at all times throughout the experiment. *Apparatus*: Cognitive behavioural training and testing was performed in the Bussey-Saksida rat touchscreen chambers (Campden Instruments Ltd, UK). Detailed description of this apparatus has been provided elsewhere (eg., [16]). Chambers were controlled using the ABET II Touch software (Lafayette Instruments) using the WhiskerServer Controller (Campden Instruments Ltd, UK).

Rodent Continuous Performance Test (rCPT): Training and testing on the rCPT was similar to that described previously [17], [18]. Testing sessions were a maximum of 60 min in duration or until an animal completed the required number of trials. Initial training comprised of four stages and animals had to individually reach criterion on each stage prior to advancing to the next one. In the first stage, rats were trained to attend, approach, and touch a solid white square stimulus presented centrally for a set stimulus duration (SD) on the touchscreen. Stimulus presentations were separated by an inter-stimulus interval (ISI) and screen touches made within the response window either while the stimulus was presented or <500ms following stimulus removal (limited hold (LH) period) were designated as hits (correct

responses). Following hits, the stimulus was removed from the screen and a single sucrose reward pellet (45 mg, BioServ) delivered to the magazine. No responses to stimuli within the LH period were classified as misses. Stage 2 introduced a novel target stimulus (S+), and Stage 3 introduced a novel nontarget stimulus (S-) to the stimulus set. Touching the S- during the LH period was designated as a false alarm (incorrect response, mistake) and resulted in immediate removal of the stimulus (if present) and initiation of a 'correction-trial' ISI. On correction trials, the same S- was presented again and these trials served to discourage nonselective responding to stimuli. Withholding responses to the S- during the LH period was designated as a correct rejection and initiated a standard-trial ISI. In the final training Stage 4, three additional S- stimuli were introduced to the stimulus set. All stimuli were luminance matched in an attempt to equate their salience for simple brightness detection. Like Stage 3, the probability of presentation of either an S+ or an S- on standard trials was equal (50%) and other parameters remained the same, with touches to any of the S- stimuli resulting in a correction trial in which an S- was presented randomly from the set of four. All animals were trained on Stage 4 to establish a plateau rCPT performance prior to receiving test sessions where task parameters (SD, stimulus contrast, ISI) were manipulated to tax attentional processing (tested in that order) (Table 1). Rats completed 2-3 test sessions on each parameter followed by 1-2 sessions on the standard parameters in between tests to re-baseline performance levels. The same training procedure was undertaken both pre-surgery and post-surgery. Based on pre-surgery performance (average d'), rats were equally allocated to Sham or ET-1 groups. Animals were given daily touchscreen training, 5-7 days a week.

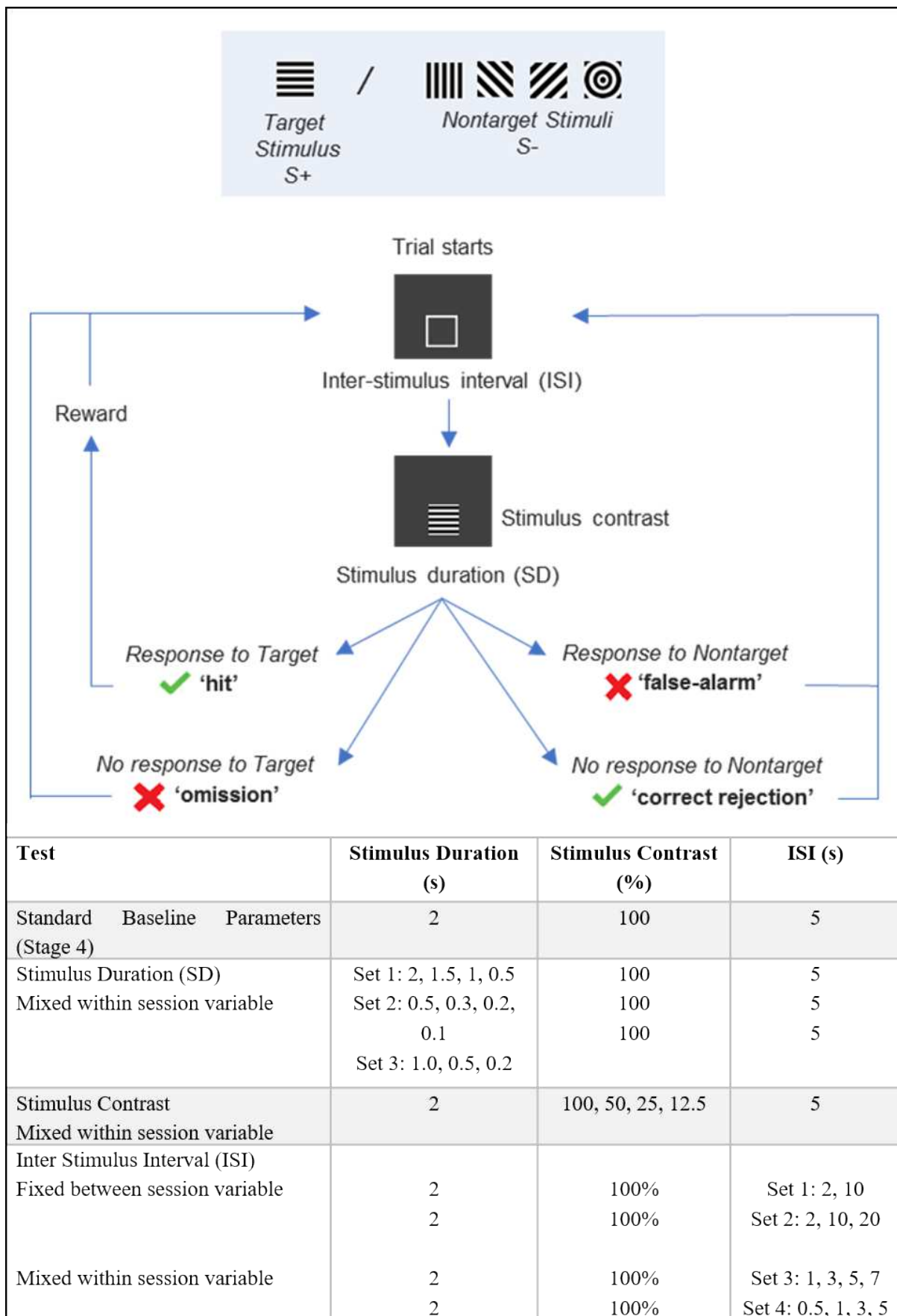


Table 1: Rodent Continuous Performance Test trial structure and parameters used to assess attentional processing (flowchart adapted from Fisher et al., 2020 [19]). For each trial, the inter-stimulus interval (ISI), stimulus contrast and/or stimulus duration (SD) can be variably manipulated. Assessment of baseline performance was measured using the standard set of parameters. To measure and probe attentional load as parameters changed, stimulus duration, stimulus contrast or inter-stimulus interval was altered either within the same test session (mixed within session variable) or across test sessions (fixed between session variable).

Behavioural Measures: Analogous to human CPTs, a response to the target (S+) was classified as a hit, failure to respond to the target was classified as a miss, withholding from responding to a nontarget (S-) was recorded as a correct rejection (CR), and responding to a nontarget was classified as a false alarm (FA). From these measures, for each animal, hit rate (HR) was calculated as the number of hits as a proportion of the total number of CS+ presentations (hits / (hits + misses). False alarm rate (FAR) was calculated as the number of false alarms as a proportion of the total number of CS- presentations (FA / (FA + CR)). The discrimination sensitivity index (d') was calculated as: $d' = z(\text{hit rate}) - z(\text{false alarm rate})$ with higher values indicating better discrimination sensitivity across the session. The response criterion was calculated as: $c = -0.5(z(\text{hit rate}) + z(\text{false alarm rate}))$ with larger values indicating decreased overall responding to both the target and nontarget stimuli. Our primary measures were discrimination sensitivity index (d'), response criterion (c), hit rate and false alarm rate. Correct response latency, incorrect response latency, and reward retrieval latency were also assessed.

Tissue processing and histological assessment

Animals were sacrificed by terminal dose of pentobarbitone (100mg/kg; Virbac, Peakhurst, Australia) and were transcardially perfused with saline followed by paraformaldehyde (PFA, 4% in 0.4M phosphate buffer with 0.2% picric acid). The brains were collected and additionally post-fixed in 4% PFA for 2 hours, followed by equilibration in 20% sucrose PBS solution for one to two days. The brains were snap frozen with dry ice prior to cutting as 40 μm coronal sections in 12 series using a freezing-microtome (Leica, Wetzlar, Germany).

Free-floating immunohistochemistry was performed on a 1:12 series for chromogenic labelling of NeuN and Ox42, or fluorescent labelling of BrdU/Prox-1, as previously described

[20]. Tissue labelled for BrdU was pre-treated by incubation in Omnipur deionized formamide (Merck Millipore) at 65°C for 2 hours, in 2M HCL at 37°C for 30 minutes and in Borate buffer at room temperature for 20 minutes. Primary antibodies and dilutions (Table 2) were: sheep anti-BrdU (Exalpa, A205P, 1:1000); rabbit anti-NeuN (Abcam, ab104225, RRID:AB_10711153, 1:1500); rabbit anti-Prox-1 (Millipore, ABN278, RRID:AB_2811075, 1:2000) and mouse anti-OX42 (Bio-Rad, MCA275GA, RRID:AB_566455, 1:200). Secondary antibodies included anti-sheep and anti-rabbit conjugated Dylight Fluorophores 488 and 555 (Jackson ImmunoResearch,1:200) for fluorescent staining and anti-rabbit and anti-mouse biotin conjugated (Jackson ImmunoResearch,1:400) for chromogenic staining.

Antibody	Immunogen	Manufacturer information	Concentration
Anti-BrdU	5-methyl cytosine (5-MeC) and bromodeoxyuridine (BrdU)	Exalpa, A205P, sheep polyclonal	1:1000
Anti-NeuN antibody - Neuronal Marker	FOX3/NeuN mouse, rat, chicken, cow, human, pig / synthetic peptide sequence not available	Abcam, ab104225, RRID:AB_10711153, rabbit polyclonal	1:1500
Anti-Prospero homeobox protein 1/PROX1 Antibody	KLH-conjugated linear peptide corresponding to the C-terminus of human Prospero homeobox protein 1/PROX1.	Millipore, ABN278, RRID:AB_2811075, rabbit polyclonal	1:2000
Mouse anti-rat CD11b/Ox42 antibody	Resident rat peritoneal macrophages.	Bio-Rad, MCA275GA, RRID:AB_566455, mouse monoclonal	1:200

Table 2: Antibody specifications.

Volumetric analysis: A 1:12 series of sections immuno-labelled for NeuN was used to quantify cortical, hippocampal and thalamic volumes at all time-points. Photomontages of whole sections were generated using a digital slide scanner (Pannoramic Scan 2, 3DHitech). Areas of the cortex, hippocampus and thalamus were measured on 14, 5 and 8 consecutive brain sections respectively, using CaseViewer 2.1 Software (3DHitech.Ltd, RRID:SCR_017654) and volumes were extrapolated using the Cavalieri principle [21].

Neuronal and microglial densities: NeuN density was calculated from one field of view image at 20x magnification (Leica DM6000) of the ipsilateral and contralateral cortices, ventral to the injury site at 1.68mm rostral to bregma. The number of NeuN+ cells in this field of view was automatically counted using ImageJ, giving a density reading. Microglial density, labelled with Ox42, was estimated at all time-points in the cortex and cerebral peduncle for ET-1 groups (both ipsilateral and contralateral) and for sham groups (ipsilateral only). One field of view was acquired using a brightfield microscope (Leica DM6000) at 40x magnification. Microglial density was assessed based on pixel intensity in Adobe Photoshop CS6. The results were reported as percentage of OX42+ pixels in one field of view for each representative region.

Statistical analysis

Statistical analysis was carried out using GraphPad Prism 8 (RRID:SCR_002798). All data are presented as mean±SD or as boxplot ± Min and Max values. An alpha of $p < 0.05$ was adopted to establish statistical significance. For touchscreen data analysis, a mixed effects model with post hoc Šídák's multiple comparisons test was performed. For histological analysis, one-way or two-way ANOVAs were adopted with post hoc Tukey's multiple comparison test. When only two groups were analysed, t-tests were adopted at each time-point. The nature of statistical testing for specific data sets is described in figure legends. All analysis, behavioural and histologic were performed blinded to group allocation.

Results

Mild ischemic injury with an asymptomatic behavioural phenotype.

Injection of ET-1 into the sensorimotor cortex of adult Long-Evans rats produced a discrete ischemic injury, evident 1 week after injection as a continuous volume of neuronal loss throughout the frontal cortex (Figure 1A). The size of the infarction was measured in coronal sections immunohistochemically labelled for NeuN as areas devoid of NeuN and extrapolated as volumes to show ET-1 produced an average lesion size of $9.51 \pm 1.86 \text{mm}^3$. This was significantly greater than damage from injection of the saline vehicle alone (Unpaired t test with Welch's correction $t(4.388) = 3.882; **p = 0.0047, n = 5$) (Figure 1B), which resulted in smaller loss of NeuN limited to the injection site.

Long-Evans rats did not display any detectable level of motor impairment in the staircase test and thus model an asymptomatic motor phenotype (Figure 1C, D). Similarly, the ischemic injury did not affect cognitive performance in a sensitive test of attentional processing and response inhibition assessed using a touchscreen-based continuous

performance test (rCPT) (Figure 2), which is analogous to human CPTs that measure the same executive processes. We found no significant difference in performance between the ET-1 and saline treated groups based on the primary measures of hit rate (Figure 2A), false alarm rate (Figure 2B), discrimination sensitivity index (Figure 2C) and response criterion or strategy (Figure 2D)(Mixed effects model: Interaction non-significant; Time factor $F_{4,199,85.38}=15.06$, $p<0.0001$; Group factor non-significant). We also assessed various response latencies (correct response, incorrect response, reward collection) during performance that serve as measures of processing speed, motivational drive and/or motoric capacity and found no changes between the ET-1 injected rats and the saline group (Supp Figures 1-5). We tested longitudinally in order to assess whether we might detect a latent development of cognitive changes, but did not find significant differences between any of the behavioural measures on our rCPT task even up to 48 weeks. These data suggest mild ischemic injury in Long-Evans rats models features relevant to human subclinical stroke.

Focal ischemic stroke induces progressive hemispheric cortical atrophy.

Characterisation of the ischemic injury over time was performed by histological analysis of serial coronal sections at 1-, 4-, 12-, 24-, 36- and 48-weeks after ET-1 injection. The infarcted area of neuronal loss was most clearly evident at 1- and 4-weeks and appeared progressive in size between these two time-points, extending into the dorsal striatum in a number of animals from the 4-week group (Figure 3). From 12-weeks the infarcted area of neuronal loss resolved around the injection site and progressed to morphological appearance resembling glial scarring that persisted up to 48-weeks. The saline injected group displayed a minor neuronal loss at the surface of the cortex corresponding to the needle injection site at 1-week, but this was resolved by 4-weeks (Figure 3).

Cortical area was measured unilaterally in coronal sections immunohistochemically labelled for NeuN in serial sections (1:12) across the rostro-caudal axis between +3.6mm and -2.64mm relative to bregma (Figure 4A). The same approach was used to measure the size of the thalamus and rostral hippocampal lobes. At 1-week post-ischemia 3 cortical levels surrounding the injury site were found to be significantly reduced in size in the ET-1 ipsilateral group (n=5) compared with the saline group (n=10)(Two-Way ANOVA: Interaction non-significant (1-, 4-, 12-, 36-week); $F_{26,266}=2.04$, $p=0.0028$ (24-week); $F_{26,294}=2.79$, $p<0.0001$ (48-week); Distance from injection site factor $F_{13,226}=13.66$, $p<0.0001$ (1-week); $F_{13,264}=28.27$, $p<0.0001$ (4-week); $F_{13,294}=36.54$, $p<0.0001$ (12-week);

$F_{13,226}=35.83$, $p<0.0001$ (24-week); $F_{13,294}=17.69$, $p<0.0001$ (36-week); $F_{13,294}=34.55$, $p<0.0001$ (48-week); Group factor $F_{2,226}=17.88$, $p<0.001$ (1-week); $F_{2,264}=53.79$, $p<0.0001$ (4-week); $F_{2,294}=111.1$, $p<0.0001$ (12-week); $F_{2,226}=100.9$, $p<0.0001$ (24-week); $F_{2,294}=51.39$, $p<0.0001$ (36-week); $F_{2,294}=37.4$, $p<0.0001$ (48-week). Tukey's multiple comparison: Supp table 1) (Figure 4B). This cortical atrophy of the ET-1 injured cortex (ipsilateral side; $n=6$), was accentuated at 4-weeks post-ischemia (Figure 4B). Around the injection site, +1.68mm from bregma, the ipsilateral ET-1 cortex was 1.5 to 2mm² smaller compared to saline ($n=10$) and to contralateral ET-1 cortex ($n=6$). This further extended caudally to -1.68mm for the contralateral side and -2.64mm for the saline injected cortex. (Tukey post hoc test: Supp Table 1).

Peak atrophy was observed at 12-weeks post-ischemia, where the ipsilateral ET-1-injected cortex ($n=6$) was 1.6-3mm² reduced in size compared with saline group ($n=12$) throughout the 14 cortical sections measured (Figure 4B). The reduction when compared to contralateral cortex of ET-1 animals was more limited, reflecting that there was also some atrophy of contralateral cortex compared to saline animals (Tukey post hoc test: Supp Table 1). This was most pronounced in the frontal cortex rostral to the injury. A similar pattern was observed at 24-weeks post-ischemia, where a reduction in cortical size was observed in the injured cortex ($n=5$) compared to saline ($n=12$), ranging from 1.6 to 2.6mm² across the 14 sections measured (Figure 4B). The ipsilateral ET-1-injected cortex was significantly smaller compared to the contralateral side around the site of injury (2mm² reduction) (Tukey post hoc test: Supp Table 1). This atrophy was stable and persistent at the long term time-points, 36- and 48-weeks post ischemia, where there remained a reduced cortical area both in ipsilateral and contralateral hemispheres of the ET-1 group ($n=6$) compared to the saline control group ($n=12$), most notably in the frontal cortex, rostral to the infarction (Figure 4B, Supp Table 1). This was reflected when represented as hemispheric cortical volume spanning +3.6 to -2.64 relative to bregma, where there was a significant reduction in ET-1 infarcted cortex from 4 weeks and persisting through to 48 weeks (Two-way ANOVA: Interaction non-significant; Time factor $F_{5,112}=7.600$, $p<0.0001$; Group factor $F_{2,112}=48.93$, $P<0.0001$; Tukey's multiple comparison: Supp Table 1) (Figure 4C). Interestingly, these measurements also showed a progressive decline in cortical volume in saline controls over time, from 4 – 48 weeks (equivalent to 24 – 68 weeks of age), corresponding to ~10% loss over that period. To assess if atrophy was associated with neuronal loss, as opposed to a collapse of extracellular volume, neuronal density was measured in an area immediately proximal to the infarction (Supp Figure 6A). Cell counting showed that neuronal density was not different between

groups (One-Way ANOVA $F_{3,16}=0.9085$ (1 week); $F_{3,18}=0.7232$ (4 week); $F_{3,20}=2,606$ (12 week); $F_{3,18}=1.935$ (24 week); $F_{3,20}=2.908$ (36 week); $F_{3,20}=0.2573$ (48 week); $n=5$) (Supp Figure 6B) and thus reduction of tissue volume represented neuronal loss. Volume of the thalamus (Figure 4A) showed no significant change between ET-1 and saline injected animals (Figure 4D; t-test at each time-point $t(10)=2.481$; $t(10)=2.437$; $t(10)=0.2177$; $t(10)=1.731$; $t(10)=1.185$; $t(10)=0.04417$. $n=6$).

Mild ischemia reduces hippocampal volume contralateral to the injury and induces cellular proliferation and neurogenesis.

Measurement of hippocampal volume showed there was no change in the ipsilateral hippocampus of ET-1 injected rats ($n=5-6$) at any time-point compared to the saline group ($n=10-12$) (Figure 5A), however there was a reduction in volume of the contralateral hippocampus ($n=5-6$), from 12-weeks, and progressing to reach statistical significance at the 36-weeks (Two-way ANOVA: Interaction non-significant; Time factor $F_{5,113}=3.436$, $p=0.0063$; Group factor $F_{2,113}=3.46$, $p=0.0348$. Tukey's multiple comparison : $p=0.0419$) (Figure 5B).

Part of our original hypothesis when embarking on this study was that mild ischemia may present as a delayed cognitive deficit at later time-points, accompanied by reduced hippocampal neurogenesis. In the contrary, we observed a robust proliferative response in the ipsilateral dorsal hippocampus, peaking at 24-weeks, that was associated with a significant increase in neurogenesis (Two-way ANOVA: Interaction $F_{6,82}=2.66$, $p=0.0208$; Time factor $F_{3,82}=22.33$, $p<0.0001$; Group factor $F_{2,82}=3.635$, $p=0.0307$; Tukey's multiple comparisons: ET-1 ipsi vs Saline $p=0.0006$; ET-1 ipsi vs ET-1 contra $p=0.0236$) (Figure 5C). The number of BrdU+/Prox1+ cells in the dentate gyrus 4 weeks after BrdU injection was increased by 2-fold in the ipsilateral hippocampus of ET-1 treated animals compared to the saline group (Two-way ANOVA: Interaction $F_{6,82}=2.449$, $p=0.0315$; Time factor $F_{3,82}=20.57$, $p<0.0001$; Group factor non-significant. Tukey's multiple comparisons: $p=0.0006$) (Figure 5D-E). There was no change in proliferation or neurogenesis in the contralateral hippocampus following ischemic injury.

Mild cortical ischemia induces long-term microglial activation in remote brain regions.

The inflammatory response induced by ET-1 focal ischemia was measured through immunohistochemical characterisation of microglia using the Ox42 antibody, which recognises the microglia-specific CR3 complement receptor (Figure 6A). A significant

microglial response, including proliferation of reactive cells with amoeboid morphology, was evident as early as 1 week after ischemia. This included a prominent level of microglial activation in and around the infarcted area but also extending dorso-ventrally throughout the injured cortical hemisphere at rostro-caudal levels closest to the injury (Figure 6A). Up-regulated microglial activity was also prominent along the ipsilateral cortico-bulbar and cortico-thalamic pathways of ET-1 treated rats, including along fibre bundles of the dorsal striatum, the globus pallidus (GP), the motor nuclei of the thalamus, the entopeduncular (EP) nucleus and the cerebral peduncle (CP) (Supp Figure 7). We observed high internal variability in microglial activation in the hippocampus ipsilateral or contralateral to the ET-1 and saline injection, which translated into absence of clear difference in microglial activation between ipsilateral and contralateral hippocampi or between ET-1 and saline groups (Supp figure 7).

To determine the longer-term impact on inflammation, microglial activation was first assessed by semi-quantitative scoring of intensity of labelling in selected regions throughout the brain at all time-points (Table 3). This showed a persistent increase in microglial activity in the ipsilateral hemisphere that was consistent across all animals up to 24-weeks after local ischemic injury, including throughout the cortico-bulbar and cortico-thalamic pathways, as well as other remote locations such as the globus pallidus (Supp Figure 7; Table 3). Inflammation in areas remote to the infarction was also evident at the later 36- and 48-week time-points but was more variable, with only around half the animals displaying increased microglial activity (Supp Figure 7). At 48-weeks microglial activation remained elevated in the ipsilateral cortex.

For a more quantitative insight into persistent microglial activation, density of Ox42 labelling was measured in the cortex and CP. Microglial activation was significantly increased in the ipsilateral cortex of ET-1 treated animals compared to the contralateral side from 1- to 36-weeks and compared to sham from 1- to 12-weeks (Two-way ANOVA: Interaction non-significant; Time factor $F_{5,84}=6.859$, $p<0.0001$; Group factor $F_{2,84}=37.99$, $p<0.0001$. Tukey's multiple comparisons: ET-1 ipsi vs Saline: $p=0.0493$, 0.0071 , 0.001 ; ET-1 ipsi vs ET-1 contra: $p=0.0015$, <0.0001 , 0.0007 , 0.0374 , 0.0026) (Figure 6B-C). In the CP, the ET-1 ipsilateral group also presented an increased microglial density compared with the contralateral side at the early time-points until 12-weeks, and compared with the saline group at 12- and 24-weeks (Two-way ANOVA: Interaction non-significant; Time factor non-significant; Group factor $F_{2,81}=24.75$, $p<0.0001$. Tukey's multiple comparisons: ET-1 ipsi vs

Saline: $p(12w) < 0.0001$, $p(24w) = 0.0051$; ET-1 ipsi vs ET-1 contra: $p(1w) = 0.0005$, $p(4w) = 0.0052$, $p(12w) = 0.0004$ (Figure 6B,D).

Regions inspected	Location relative to Bregma (mm)	1 week	4 weeks	12 weeks	24 weeks	36 weeks	48 weeks
Cortex	+1.70	++	++	++	+	+	+
Dorsal striatum	+1.70	++	++	++	+	+	/
Hippocampus	-3.0	+/	+/	+/	+/	+/	+/
Thalamus	-3.6	++	++	++	+	++	/
Entopeduncular nucleus (EP)	-2.8	++	++	++	++	++	/
Cerebral peduncle	-4.8	++	+	++	++	+	/
Globus pallidus	-0.92	++	++	++	+	++	/

Table 3: Qualitative comparison of microglial density at high magnification for all time-points, of the ipsilateral hemisphere of ET-1 injected rats compared to saline injected rats.

“++” represents a strong increase in microglial density in the ET-1 group compared with saline and “+” representing a smaller increase and “/” represents no qualitative difference between the groups. “+/” indicates variable ranging from a small increase to no change.

Discussion

These results show that modelling of mild, asymptomatic ischemic injury in rats leads to significant histopathological outcomes, including diffuse atrophy of the ipsilesional cortex and a chronic inflammatory response persisting for almost a year after the infarction. Animal modelling of human stroke has overwhelmingly focussed on severe forms, with analysis of the functional and histopathological outcomes generally limited to the sub-acute phase up to a few weeks after injury [22]–[26]. However, stroke is highly heterogenous with respect to severity and there is increasing evidence to suggest that more moderate forms, including

subclinical stroke, can lead to significant brain changes with delayed behavioural and cognitive decline manifesting much later in the chronic phase after injury [4], [27], [28].

We found that the Long-Evans rats did not display any detectable level of motor impairment in the staircase test. We interpret this as modelling an asymptomatic stroke phenotype. Similarly, the ischemic injury did not affect cognitive performance in a sensitive test of executive function assessed using a touchscreen apparatus. We have previously reported that the same ET-1 injection procedure in athymic rats resulted in focal cortical ischemic injury with similar size ($9.0 \pm 2.7 \text{mm}^3$) and a robust deficit in skilled forelimb use as revealed by pellet retrieval in the staircase test [13]. The development of a focal ischemic injury after injection of ET-1 into the sensorimotor cortex is consistent with findings from previous studies [29]–[31], including our own recent work in athymic rats [13]. Interestingly, the resulting impairment of skilled forelimb function seen in T-Cell deficient, athymic rats was not observed here when using the same procedures on Long Evans rats, highlighting strain-dependent differences for the threshold for impairment of motor function following mild ischemic injury. This may also be related to a role of the immune system in the development of injury and impairment. Previous studies have suggested a beneficial role for T-cells in the chronic phase after infarction, e.g. through clearance of cellular debris [32], and thus the lack of this process may contribute to the greater sensitivity to injury in athymic animals. In addition to a lack of impact on motor function in the present study in Long Evans rats, we did not observe any impact of the injury on attentional processing in a complex touchscreen-based test, a cognitive ability often impaired following stroke [33]. This injury model thus approximates more mild forms of human stroke, such as asymptomatic or subclinical stroke, compared to other commonly used pre-clinical models that produce large ischemic infarction associated with robust deficits in motor and/or cognitive function in the acute phase after injury [23], [25], [26], [34].

Despite the mild nature of the initial injury, there followed a significant and progressive atrophy across the entire ipsilateral cortical hemisphere, including rostral and caudal levels remote to the site of injury. The atrophy was progressive up to 12 weeks and maintained up to 48 weeks, representing $\sim 10\%$ loss in cortical volume compared to controls. The progressive cortical thinning in the sham animals was also interesting to note, as thinning of the cortex with healthy aging has been reported in humans, with an annual decline of 0.5%, and an accelerated rate in diseased brains such as those suffering from Alzheimer disease [35], [36]. Quantification of neuronal density showed that atrophy represented

neuronal loss and not shrinkage of the extra-cellular compartment. This is consistent with our recent observations using the same model of injury in athymic rats [13].

Progressive atrophy remote to the site of infarction is increasingly becoming recognised as an important feature of stroke pathophysiology. Recent clinical imaging studies have reported whole brain, hemispheric and nuclei-specific atrophy following stroke, with rapid progression in the first 6 months [37] and persisting for years after the injury [38], [39]. The relationship between the development of dementia after stroke and progression of atrophy in brain regions remote to the site of damage is becoming an increasingly important area [40]. It is thus important to consider that even mild strokes, initially appearing asymptomatic or with transient symptoms, may trigger a progressive atrophy as the substrate for cognitive decline later in life. Given we did not observe deficits in attentional processing in the present study, it will be important to investigate other cognitive domains in order to establish a model linking brain atrophy to cognitive decline. It should also be noted that the acute injury was targeted unilaterally to the motor cortex. Deficits in cognitive function are more likely to arise after damage to other cortical areas as previously shown following bilateral focal ischemic injury to prefrontal cortex [41], [42]. Age of infarction may also be an important factor. Clinical studies showing mild strokes such as single microinfarcts are associated with subtle cognitive decline have been largely based on observations in older patients [5], [43].

Measures of other brain structures such as thalamus and hippocampus did not reveal additional areas of remote atrophy. This is in contrast to other rodent [44], [45], [23], [46] and clinical imaging studies [22], [37], [47], [48], and may reflect a threshold level of severity of the initial injury required for involvement of secondary atrophy in remote structures beyond the cortex. Indeed, previous observations of reductions in contralesional thalamic volume have indicated that the degree of atrophy is proportional to the severity of stroke [49], [50].

On the basis of our original hypothesis that the cortical infarction may precipitate an ipsilesional hippocampal atrophy with accompanying cognitive deficit, we were interested to assess if there was an accompanying decrease in hippocampal neurogenesis as a correlative feature. Interestingly we observed the opposite, where there was an overall proliferative response and transient increase in hippocampal neurogenesis. A recent study using a series of immunohistochemical analyses of human biopsy tissue from stroke patients, has shown the first evidence of stroke-induced neurogenesis in humans [51]. This is consistent with studies of rodent brain injury including both epilepsy [52] and stroke [53] where both reports show an increase in hippocampal neurogenesis but aberrant functional integration of new neurons

generated in an inflammatory environment. The study by Voitke et al concluded that ischemia-induced maladaptive plasticity may be a contributing factor to the accompanying cognitive impairment [53]. While we did not directly assess function of the new neurons here, the results are nonetheless significant in that they show that mild stroke can affect fundamental aspects of physiology in remote brain areas as potentially contributing factors to clinical outcome and thus targets for therapy.

Inflammation is a universal response to stroke that has been well described clinically and in animal models as a target for therapeutic intervention [54], [55]. The vast majority of these studies have limited their analyses to the acute and sub-acute period after injury, i.e. days or weeks after large strokes [56]–[58]. Here we show that even a mild, localised ischemic injury can produce a diffuse and chronic inflammatory response throughout the ipsilesional cortex and also in remote brain areas persisting up to 48 weeks. Microglial activation along striatal fibre bundles, entopeduncular nucleus and cerebral peduncle likely represents axonal degeneration of the cortico-bulbar projection pathway. Inflammation in other areas may represent die-back of afferently connected nuclei and/or diffusion of inflammatory cytokines from the infarcted area, for example through the ipsilateral cortex. While interventions aimed at reducing inflammation after stroke have shown to be effective in the acute phase [59]–[61], less is known about the impact of chronic inflammation and how it might relate to progressive atrophy and latent cognitive decline as an additional therapeutic target. The present results provide a platform for further investigation in this area.

In summary, these results show that modelling of mild, focal ischemic injury in rats produces significant and long-lasting histopathological outcomes despite a lack of obvious impact on motor or cognitive function. Our evolving understanding of the heterogeneity of stroke pathophysiology and the relationship to clinical outcome demands parallel development of animal models that capture different elements of human stroke. This is particularly true at the milder end of the spectrum, where there is rapidly building evidence that the clinical burden associated with mild forms of stroke may be greater than previously recognised. The present results highlight that atrophy and inflammation are interesting targets for therapeutic intervention in the chronic phase after mild stroke in rats.

Study limitation: Due to logistical limitations (i.e. housing of animals limitation for the duration of the study and personnel limitation to handle a cohort double the current size (190 rats)), only males were used in this study. It should be noted, however, that studying sex-

dependent effects will be important for future work. Although the age of rats at 22 weeks is older than those used in most stroke modelling studies, these animals are still regarded physiologically as ‘young adult’, whereas stroke is more common in older patients.

Acknowledgements: The authors thank Mong Tien for expert technical assistance in the tissue preparation and immunohistochemical procedures. The Florey Institute of Neuroscience and Mental Health acknowledges the strong support from the Victorian Government and in particular the funding from the Operational Infrastructure Support Grant.

Author contributions: C.E., K.O., J.K., S.F. and A.O. contributed to the experimental procedures and C.E. and K.O. to the analysis. C.E., J.N., V.B., A.B., and L.T. contributed to the conception and design of the study. L.T. and C.E. wrote the manuscript and constructed the figures. L.T., J.N., M.P. and A.B. sourced funding for the work. All authors contributed to manuscript revision and editing and approved the submitted version.

Data and Materials Accessibility: Requests for further information or biological data and reagents should be directed to and will be fulfilled by charlotte.ermine@florey.edu.au or lachlant@unimelb.edu.au

Figure legends

Figure 1. *Mild ischemic injury with cortical infarction and lack of robust motor deficit. A)* Representative coronal sections immunolabelled for the neuronal marker NeuN shows the infarcted area as absence of neurons 1 week after ET-1 treatment. **B)** The average infarcted volume was significantly greater in the ET-1 compared to saline group (Unpaired t test with Welch’s correction $t(4.388)=3.882; *p=0.0149, n=5$). **C-D)** The staircase test is a sensitive measure of skilled forelimb use and at 4 weeks showed no difference in performance between the ET-1 and saline treated groups for the relative (C) or absolute (D) number of pellets retrieved with the left or right forelimbs (Saline $n=9$; ET-1 $n=13$). All data shown as boxplot \pm Min and Max values. Scale bar: A, 500 μ m.

Figure 2. *Attentional processing as a measure of cognitive performance after mild ischemic injury.* A rodent touchscreen-based Continuous Performance Test (rCPT) to assess attentional processing showed no difference in performance between the ET-1 and saline treated groups

on a range of parameters, including: **A)** Hit Rate, **B)** False Alarm Rate, **C)** Discrimination Sensitivity Index (d') and **D)** Response Criterion (Pre-Stroke to 36 weeks: Saline n=10; 48 weeks: Saline n=9; Pre-Stroke to 12 weeks: ET-1 n=13; 24 to 48 weeks: ET-1 n=12; Mixed effects model: Interaction non-significant; Time factor $F_{4,199, 85.38}=15.06$, $p<0.0001$; Group factor non-significant) All data shown as boxplot \pm Min and Max values.

Figure 3. Longitudinal assessment of cortical infarction following focal ischemic injury. Immunohistochemistry for NeuN in representative coronal sections at the level of ET-1 or saline injection illustrates gross morphology and the progression of the ischemic infarction 1-, 4-, 12-, 24-, 36- and 48-weeks following treatment. Scale bar: 500 μ m.

Figure 4. Progressive cortical atrophy up to 48 weeks following focal ischemia. **A)** Colour overlays on representative coronal sections illustrate anatomical boundaries used to quantify area for specific brain regions. **B)** Cortical area measured at each of 14 coronal sections from 3.6mm rostral to 2.64mm caudal to bregma showed a progressive and significant atrophy of the cortex both proximal and remote to the infarction and including both the ipsilateral and contralateral hemispheres (Two-Way ANOVA: Interaction non-significant (1-, 4-, 12-, 36-week); $F_{26,266}=2.04$, $p=0.0028$ (24-week); $F_{26,294}=2.79$, $p<0.0001$ (48-week); Distance from injection site factor $F_{13,226}=13.66$, $p<0.0001$ (1-week); $F_{13,264}=28.27$, $p<0.0001$ (4-week); $F_{13,294}=36.54$, $p<0.0001$ (12-week); $F_{13,226}=35.83$, $p<0.0001$ (24-week); $F_{13,294}=17.69$, $p<0.0001$ (36-week); $F_{13,294}=34.55$, $p<0.0001$ (48-week); Group factor $F_{2,226}=17.88$, $p<0.001$ (1-week); $F_{2,264}=53.79$, $p<0.0001$ (4-week); $F_{2,294}=111.1$, $p<0.0001$ (12-week); $F_{2,226}=100.9$, $p<0.0001$ (24-week); $F_{2,294}=51.39$, $p<0.0001$ (36-week); $F_{2,294}=37.4$, $p<0.0001$ (48-week). Tukey's multiple comparison * $p<0.05$, ** $p<0.01$, *** $p<0.001$, **** $p<0.0001$. n=5-6). **C)** Hemispheric cortical volume spanning +3.6 to -2.64 relative to bregma was significantly reduced in the ipsilateral hemisphere from 4 weeks and persisting up to 48 weeks (Two-way ANOVA: Interaction non-significant; Time factor $F_{5,112}=7.600$, $p<0.0001$; Group factor $F_{2,112}=48.93$, $P<0.0001$. Tukey's multiple comparison * $p<0.05$, ** $p<0.01$, *** $p<0.001$, **** $p<0.0001$. N=5-6). **D)** Thalamic volume was not significantly changed by ET-1-induced ischemia up to 48-weeks. (t-test at each time-point $t(10)=2.481$; $t(10)=2.437$; $t(10)=0.2177$; $t(10)=1.731$; $t(10)=1.185$; $t(10)=0.04417$. n=6). All data shown as the group mean \pm SD. Scale bar: I, 1mm.

Figure 5. *Contralateral hippocampal volume loss and increased neurogenesis following ET-1 induced ischemia.* **A)** Colour overlays on representative coronal sections illustrate anatomical boundaries used to quantify the dorsal hippocampus. **B)** Quantification of dorsal hippocampal volume showed a moderate but stable reduction in the contralateral hippocampus relative to the ipsilateral hemisphere, reaching significance at 36-weeks post-ischemia (Two-way ANOVA: Interaction non-significant; Time factor $F_{5,113}=3.436$, $p=0.0063$; Group factor $F_{2,113}=3.46$, $p=0.0348$. Tukey's multiple comparison $*p=0.0419$, $n=5-6$). **C)** The number of BrdU+ cells was significantly higher in the ipsilateral dentate gyrus of ET-1 treated rats compared with both contralateral ET-1 and Saline treated rats at 24 weeks post-ischemia (Two-way ANOVA: Interaction $F_{6,82}=2.66$, $p=0.0208$; Time factor $F_{3,82}=22.33$, $p<0.0001$; Group factor $F_{2,82}=3.635$, $p=0.0307$; Tukey's multiple comparisons, $*p=0.0236$, $***p=0.0006$, $n=6$). **D)** Representative image of immunohistochemistry for BrdU and Prox1 in the dentate gyrus with boxed insets at higher magnification showing 2 cells double labelled for BrdU and Prox1. **E)** Cell counting showed that the number of BrdU+/Prox1+ cells was significantly increased at 24-weeks post-ischemia in the dentate gyrus of ET-1 ipsilateral group compared with the saline group (Two-way ANOVA: Interaction $F_{6,82}=2.449$, $p=0.0315$; Time factor $F_{3,82}=20.57$, $p<0.0001$; Group factor non-significant. Tukey's multiple comparisons, $***p=0.0006$, $n=6$). All data shown as the group mean \pm SD. Scale bar: A, 1mm, D, 100 μ m (50 μ m inset).

Figure 6. *Chronic and remote microglial activation following focal ischemic injury.* **A)** Immunohistochemistry for Ox42 in serial coronal sections in a representative example from 1 week and 24 weeks after injury shows the inflammatory response at acute and chronic phases after injury, respectively. **B)** High magnification images of immunohistochemistry for Ox42 in the cortex and cerebral peduncle (CP) of ET-1 injected animals at 1-, 4-, 12-, 24-, 36- and 48-weeks post-ischemia shows persistence of microglial activation over time, relative to saline controls. This was quantified by optical density measurements and showed a significant increase in microglial density up to 36 weeks in the cortex **C)**; Two-way ANOVA: Interaction non-significant; Time factor $F_{5,84}=6.859$, $p<0.0001$; Group factor $F_{2,84}=37.99$, $p<0.0001$. Tukey's multiple comparisons, $*p<0.05$, $**p<0.01$, $***p<0.001$, $n=5-6$) and up to 24 weeks in the CP **D)**; Two-way ANOVA: Interaction non-significant; Time factor non-significant; Group factor $F_{2,81}=24.75$, $p<0.0001$. Tukey's multiple comparisons, $**p<0.01$, $***p<0.001$, $****p<0.0001$, $n=5-6$.) All data shown as boxplot \pm Min and Max values. Scale bar: A, 1mm and B, 50 μ m.

Table 1. Rodent Continuous Performance Test parameters used to assess attentional processing.

Table 2: Antibody specifications.

Table 3. Qualitative comparison of microglial density at high magnification for all time-points, of the ipsilateral hemisphere of ET-1 injected rats compared to saline injected rats. “++” represents a strong increase in microglial density in the ET-1 group compared with saline and “+” representing a smaller increase and “/” represents no qualitative difference between the groups. +/- indicates variable ranging from a small increase to no change.

References

- [1] F. Fluri, M. K. Schuhmann, and C. Kleinschnitz, “Animal models of ischemic stroke and their application in clinical research,” *Drug Des. Devel. Ther.*, vol. 9, pp. 3445–3454, 2015.
- [2] A. Canazza, L. Minati, C. Boffano, E. Parati, and S. Binks, “Experimental models of brain ischemia: a review of techniques, magnetic resonance imaging, and investigational cell-based therapies,” *Front. Neurol.*, vol. 5, p. 19, Feb. 2014.
- [3] S. Prabhakaran *et al.*, “Prevalence and determinants of subclinical brain infarction The Northern Manhattan Study,” *Neurology*, vol. 70, pp. 425–430, 2008.
- [4] C. Lei, Q. Deng, and H. Li, “Association Between Silent Brain Infarcts and Cognitive Function : A Systematic Review and Meta-Analysis,” *J. Stroke Cerebrovasc. Dis.*, vol. 28, no. 9, pp. 2376–2387, 2019.
- [5] M. S. Dhamoon *et al.*, “Functional trajectories, cognition, and subclinical cerebrovascular disease,” *Stroke*, vol. 49, no. 3, pp. 549–555, 2019.
- [6] S. C. Johnston *et al.*, “Prevalence and knowledge of transient ischemic attack among US adults,” 2003.
- [7] J. B. Leverenz, K. S. Montine, C. R. Jack, J. Kaye, and K. Lim, “Ecology of the Aging Human Brain,” *Arch Neurol*, vol. 68, no. 8, pp. 1049–1056, 2011.
- [8] E. Pedrono *et al.*, “An optimized mouse model for transient ischemic attack.,” *J.*

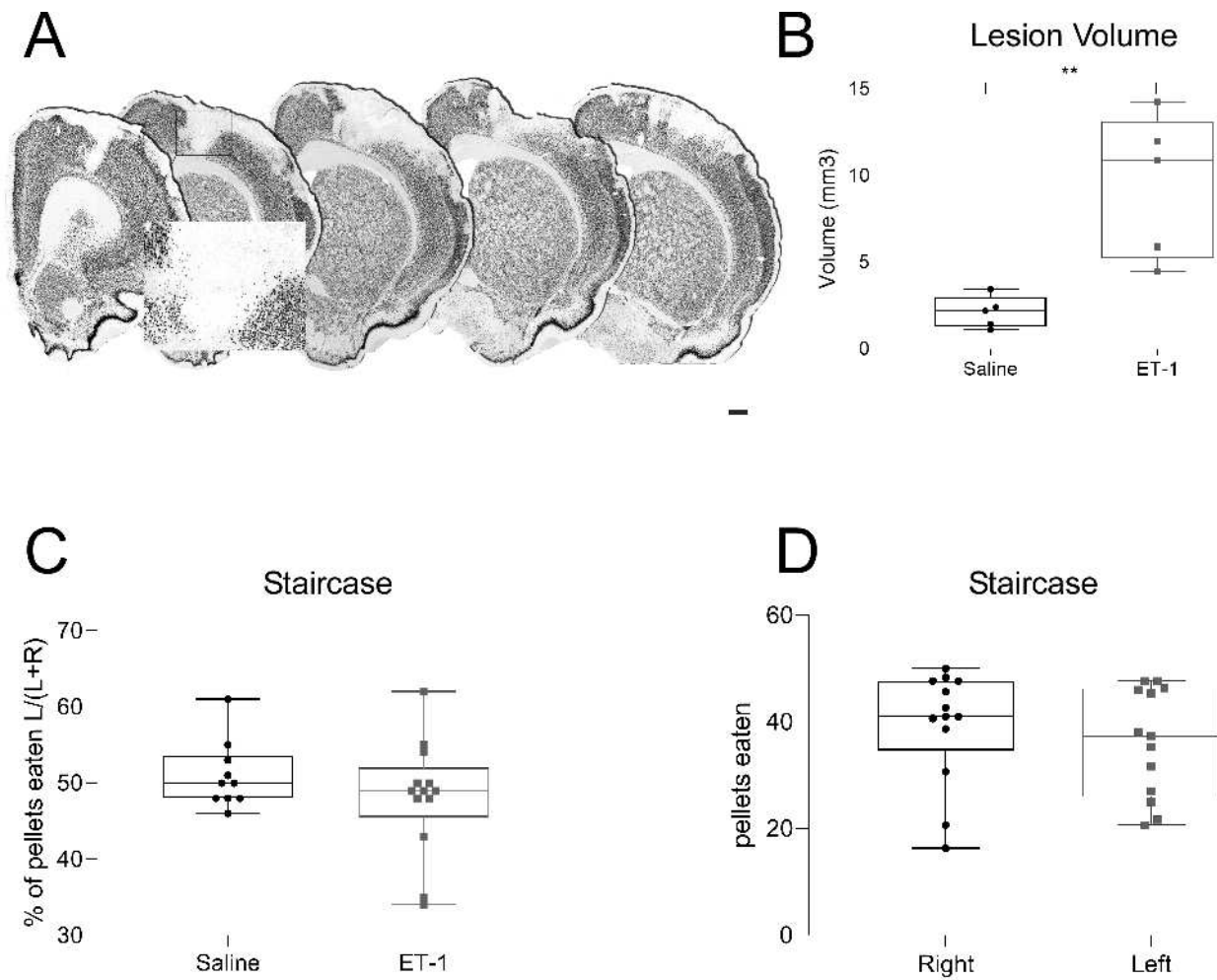
- Neuropathol. Exp. Neurol.*, vol. 69, no. 2, pp. 188–195, Feb. 2010.
- [9] D. M. Hermann, E. Kilic, R. Hata, K. A. Hossmann, and G. Mies, “Relationship between metabolic dysfunctions, gene responses and delayed cell death after mild focal cerebral ischemia in mice,” *Neuroscience*, vol. 104, no. 4, pp. 947–955, 2001.
- [10] F. Ouyang *et al.*, “Neuronal loss without amyloid- β deposits in the thalamus and hippocampus in the late period after middle cerebral artery occlusion in cynomolgus monkeys,” vol. 0, pp. 1–14, 2019.
- [11] H.-W. Nah *et al.*, “New brain infarcts on magnetic resonance imaging after coronary artery bypass graft surgery: lesion patterns, mechanism, and predictors,” *Ann. Neurol.*, vol. 76, no. 3, pp. 347–355, Sep. 2014.
- [12] H. C. S. Abeysinghe and C. L. Roulston, “A Complete Guide to Using the Endothelin-1 Model of Stroke in Conscious Rats for Acute and Long-Term Recovery Studies,” *Methods Mol. Biol.*, vol. 1717, pp. 115–133, 2018.
- [13] C. M. Ermine *et al.*, “Long-Term Motor Deficit and Diffuse Cortical Atrophy Following Focal Cortical Ischemia in Athymic Rats,” vol. 13, no. December, 2019.
- [14] C. P. Montoya, L. J. Campbell-Hope, K. D. Pemberton, and S. B. Dunnett, “The “staircase test” a measure of independent forelimb reaching and grasping abilities in rats,” *J. Neurosci. Methods*, vol. 36, pp. 219–228, 1991.
- [15] C. Winkler, C. Bentlage, G. Nikkhah, M. Samii, and A. Bjö, “Intranigral Transplants of GABA-Rich Striatal Tissue Induce Behavioral Recovery in the Rat Parkinson Model and Promote the Effects Obtained by Intrastratial Dopaminergic Transplants,” vol. 186, pp. 165–186, 1999.
- [16] A. C. Mar *et al.*, “The touchscreen operant platform for assessing executive function in rats and mice,” vol. 8, no. 10, pp. 1985–2005, 2013.
- [17] C. H. Kim *et al.*, “The continuous performance test (rCPT) for mice : a novel operant touchscreen test of attentional function,” pp. 3947–3966, 2015.
- [18] A. C. Mar *et al.*, “MAM-E17 rat model impairments on a novel continuous performance task : effects of potential cognitive enhancing drugs,” pp. 2837–2857, 2017.
- [19] B. M. Fisher, L. Sakisida, T. Robbins, and T. Bussey, “Functional Dissociations Between Subregions of the Medial Prefrontal Cortex on the Rodent Touchscreen Continuous Performance Test (rCPT) of Attention,” *Behav. Neurosci.*, vol. 134, no. 1, pp. 1–14, 2020.
- [20] C. M. Ermine *et al.*, “Modelling the dopamine and noradrenergic cell loss that occurs

- in Parkinson ' s disease and the impact on hippocampal neurogenesis,” no. September 2017, pp. 327–337, 2018.
- [21] B. Cavalieri, “Geometria degli indivisibil,” 1966.
- [22] W. Wang, C. Redecker, and O. W. Witte, “Delayed neuronal death and damage of GDNF family receptors in CA1 following focal cerebral ischemia,” vol. 1023, pp. 92–101, 2004.
- [23] E. R. Zanier *et al.*, “Six-Month Ischemic Mice Show Sensorimotor and Cognitive Deficits Associated with Brain Atrophy and Axonal Disorganization,” *CNS Neurosci. Ther.*, vol. 19, pp. 695–704, 2013.
- [24] S. S. J. Rewell *et al.*, “Evolution of ischemic damage and behavioural deficit over 6 months after MCAo in the rat : Selecting the optimal outcomes and statistical power for multi-centre preclinical trials,” pp. 1–19, 2017.
- [25] W. Li *et al.*, “Transient focal cerebral ischemia induces long-term cognitive function deficit in an experimental ischemic stroke model,” *Neurobiol. Dis.*, vol. 59, pp. 18–25, Nov. 2013.
- [26] H. Kimihiko, L. Hanna, H. P. D., C. B. J., T. R. J., and D. A. Courtney, “Cognitive Deficits After Focal Cerebral Ischemia in Mice,” *Stroke*, vol. 31, no. 8, pp. 1939–1944, Aug. 2000.
- [27] P. S. T., W. Sarah, S. L. E., M. Ziyah, and R. P. M., “Transient Cognitive Impairment in TIA and Minor Stroke,” *Stroke*, vol. 42, no. 11, pp. 3116–3121, Nov. 2011.
- [28] F. G. Van Rooij *et al.*, “Persistent Cognitive Impairment After Transient Ischemic Attack,” *Stroke*, vol. 45, pp. 2270–2274, 2014.
- [29] G. Gilmour, S. D. Iversen, M. F. O. Neill, and D. M. Bannerman, “The effects of intracortical endothelin-1 injections on skilled forelimb use : implications for modelling recovery of function after stroke,” vol. 150, pp. 171–183, 2004.
- [30] S. Soleman, P. Yip, J. L. Leasure, and L. Moon, “Sustained sensorimotor impairments after endothelin-1 induced focal cerebral ischemia (stroke) in aged rats,” *Exp. Neurol.*, vol. 222, no. 1, pp. 13–24, 2010.
- [31] V. Windle *et al.*, “An analysis of four different methods of producing focal cerebral ischemia with endothelin-1 in the rat.,” *Exp. Neurol.*, vol. 201, no. 2, pp. 324–334, Oct. 2006.
- [32] U. M. Selvaraj and A. M. Stowe, “Long-term T cell responses in the brain after an ischemic stroke,” *Discov. Med.*, vol. 24, no. 134, pp. 323–333, Dec. 2017.
- [33] T. B. Cumming, R. S. Marshall, and R. M. Lazar, “Stroke, cognitive deficits, and

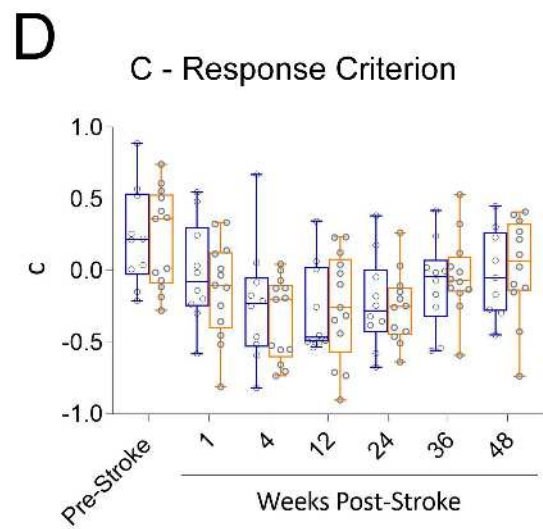
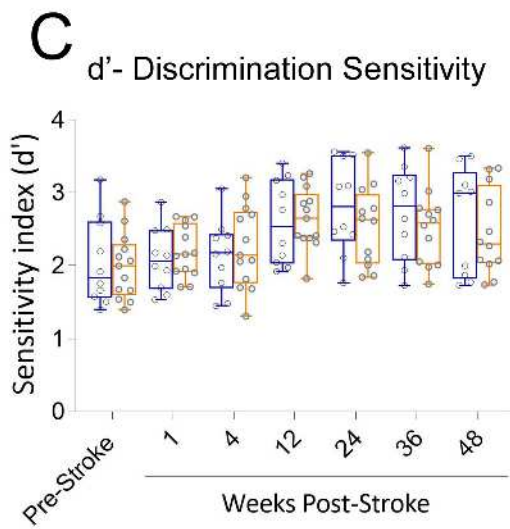
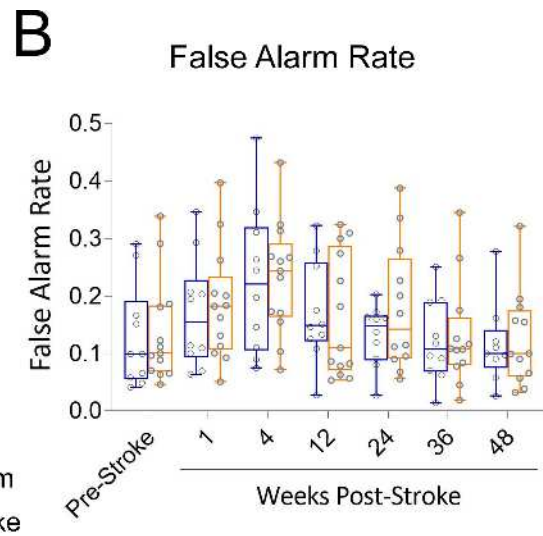
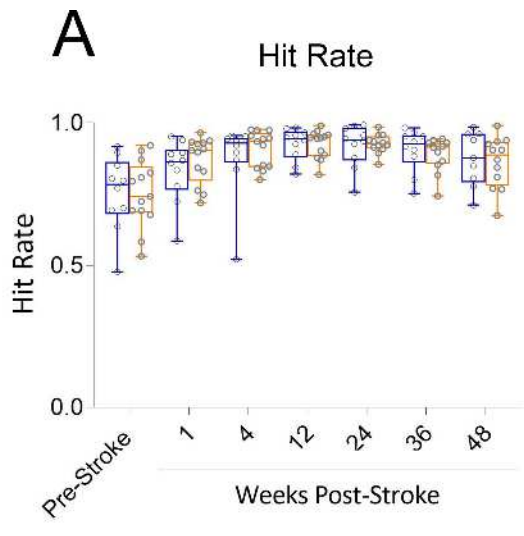
- rehabilitation: still an incomplete picture.,” *Int. J. stroke Off. J. Int. Stroke Soc.*, vol. 8, no. 1, pp. 38–45, Jan. 2013.
- [34] F. Fluri, M. K. Schuhmann, and C. Kleinschnitz, “Animal models of ischemic stroke and their application in clinical research,” *Drug Des. Devel. Ther.*, vol. 9, pp. 3445–3454, Jul. 2015.
- [35] A. M. Fjell *et al.*, “One-Year Brain Atrophy Evident in Healthy Aging,” vol. 29, no. 48, pp. 15223–15231, 2009.
- [36] D. H. Salat *et al.*, “Thinning of the Cerebral Cortex in Aging,” no. July, pp. 721–730, 2004.
- [37] A. Brodtmann, M. Khelif, N. Egorova, M. Veldsman, L. Bird, and E. Werden, “Dynamic regional brain atrophy rates in the first year after ischemic stroke,” *Stroke*, vol. In Press.
- [38] M. L. Seghier, S. Ramsden, L. Lim, A. P. Leff, and C. J. Price, “Gradual Lesion Expansion and Brain Shrinkage Years After Stroke,” *stroke*, vol. 45, pp. 877–879, 2014.
- [39] A. Bivard *et al.*, “Transient Ischemic Attack Results in Delayed Brain Atrophy and Cognitive Decline,” *Stroke*, vol. 49, no. 2, pp. 384–390, 2018.
- [40] J.-H. Sun, L. Tan, and J.-T. Yu, “Post-stroke cognitive impairment: epidemiology, mechanisms and management,” *Ann. Transl. Med.*, vol. 2, no. 8, p. 80, Aug. 2014.
- [41] C. A. Cordova, D. Jackson, K. D. Langdon, K. A. Hewlett, and D. Corbett, “Impaired executive function following ischemic stroke in the rat medial prefrontal cortex.,” *Behav. Brain Res.*, vol. 258, pp. 106–111, Jan. 2014.
- [42] L. Y. Y. Zhou, T. E. Wright, and A. N. Clarkson, “Prefrontal cortex stroke induces delayed impairment in spatial memory.,” *Behav. Brain Res.*, vol. 296, pp. 373–378, Jan. 2016.
- [43] W. T. Longstreth *et al.*, “Defined by Serial Cranial Magnetic Resonance Imaging in the Elderly The Cardiovascular Health Study,” pp. 2376–2382, 2002.
- [44] W. Fujie, T. Kirino, N. Tomukai, T. Iwasawa, and A. Tamura, “Progressive Shrinkage of the Thalamus Following Middle Cerebral Artery Occlusion in Rats,” pp. 1485–1488, 1990.
- [45] H. Iizuka, K. Sakatani, and W. Young, “Neural Damage in the Rat Thalamus After Cortical Infarcts,” *Stroke*, vol. 21, no. 5, pp. 790–794, 1990.
- [46] B. McDaniel, H. Sheng, D. S. Warner, L. W. Hedlund, and H. Benveniste, “Tracking Brain Volume Changes in C57BL / 6J and ApoE-Deficient Mice in a Model of

- Neurodegeneration : A 5-Week Longitudinal Micro-MRI Study,” vol. C, pp. 1244–1255, 2001.
- [47] M. Xie, C. Yi, X. Luo, S. Xu, and Z. Yu, “Glial Gap Junctional Communication Involvement in Hippocampal Damage After Middle Cerebral Artery Occlusion,” pp. 121–132, 2011.
- [48] P. Schaapsmeeders *et al.*, “Ipsilateral Hippocampal Atrophy Is Associated With Long-Term Memory Dysfunction After Ischemic Stroke in Young Adults,” vol. 2442, no. February, pp. 2432–2442, 2015.
- [49] A. Brodtmann, H. Pardoe, Q. Li, R. Lichter, L. Ostergaard, and T. Cumming, “Changes in regional brain volume three months after stroke,” *J. Neurol. Sci.*, vol. 322, no. 1, pp. 122–128, 2012.
- [50] N. Yassi *et al.*, “Contralesional Thalamic Surface Atrophy and Functional Disconnection 3 Months after Ischemic Stroke,” vol. 3050, pp. 232–241, 2015.
- [51] K. Jin *et al.*, “Evidence for stroke-induced neurogenesis in the human brain.,” *Proc. Natl. Acad. Sci. U. S. A.*, vol. 103, no. 35, pp. 13198–202, 2006.
- [52] K. Jakubs *et al.*, “Environment matters: synaptic properties of neurons born in the epileptic adult brain develop to reduce excitability.,” *Neuron*, vol. 52, no. 6, pp. 1047–1059, Dec. 2006.
- [53] F. Woitke *et al.*, “Adult hippocampal neurogenesis poststroke: More new granule cells but aberrant morphology and impaired spatial memory.,” *PLoS One*, vol. 12, no. 9, p. e0183463, 2017.
- [54] R. L. Jayaraj, S. Azimullah, R. Beiram, F. Y. Jalal, and G. A. Rosenberg, “Neuroinflammation: friend and foe for ischemic stroke.,” *J. Neuroinflammation*, vol. 16, no. 1, p. 142, Jul. 2019.
- [55] K. Shi, D.-C. Tian, Z.-G. Li, A. F. Ducruet, M. T. Lawton, and F.-D. Shi, “Global brain inflammation in stroke,” *Lancet. Neurol.*, vol. 18, no. 11, pp. 1058–1066, 2019.
- [56] T. Morioka, A. N. Kalehua, W. J. Streit, N. Surgery, and A. N. K. Neuroscience, “Characterization of Microglial Reaction After Middle Cerebral Artery Occlusion in Rat Brain,” vol. 132, 1993.
- [57] C. J. S. Price *et al.*, “Intrinsic activated microglia map to the peri-infarct zone in the subacute phase of ischemic stroke.,” *Stroke*, vol. 37, no. 7, pp. 1749–1753, Jul. 2006.
- [58] N. Gorlamandala *et al.*, “Focal Ischaemic Infarcts Expand Faster in Cerebellar Cortex than Cerebral Cortex in a Mouse Photothrombotic Stroke Model,” pp. 643–653, 2018.
- [59] R. Jin, G. Yang, and G. Li, “Inflammatory mechanisms in ischemic stroke : role of

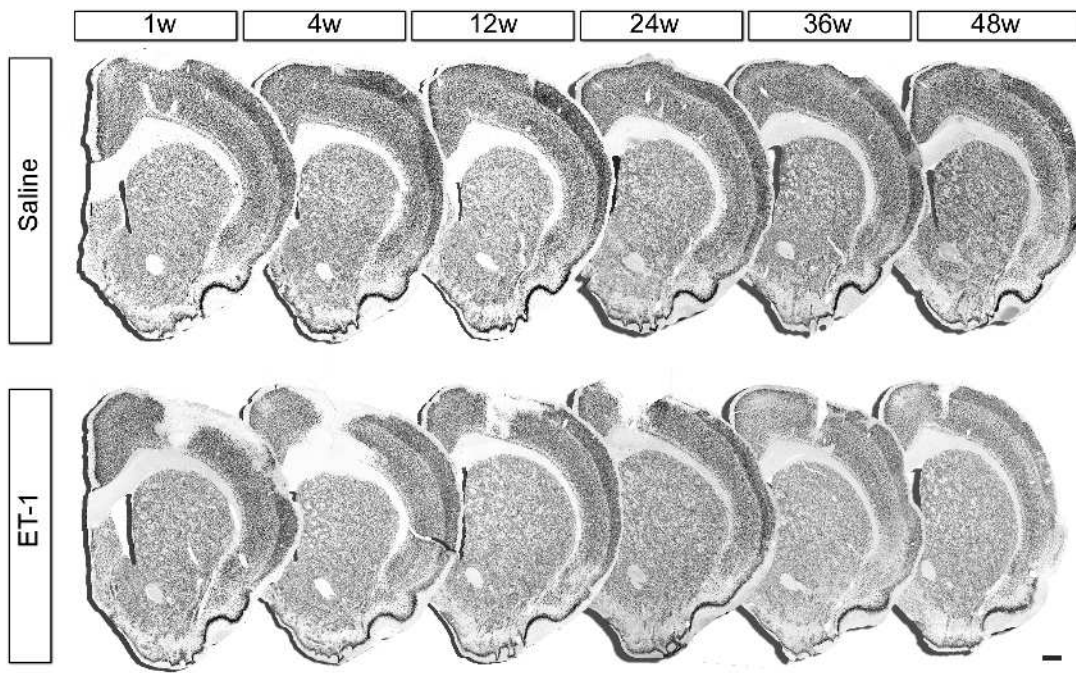
- inflammatory cells,” *J. Leukoc. Biol.*, vol. 87, pp. 779–789, 2010.
- [60] K. L. Lambertsen, B. Finsen, and B. H. Clausen, “Post-stroke inflammation — target or tool for therapy ?,” *Acta Neurol. (Napoli)*., vol. 137, pp. 693–714, 2019.
- [61] M. Ahmad and S. H. Graham, “Inflammation After Stroke: Mechanisms and Therapeutic Approches,” *Transl. Neurodegener.*, vol. 1, no. 2, pp. 74–84, 2010.



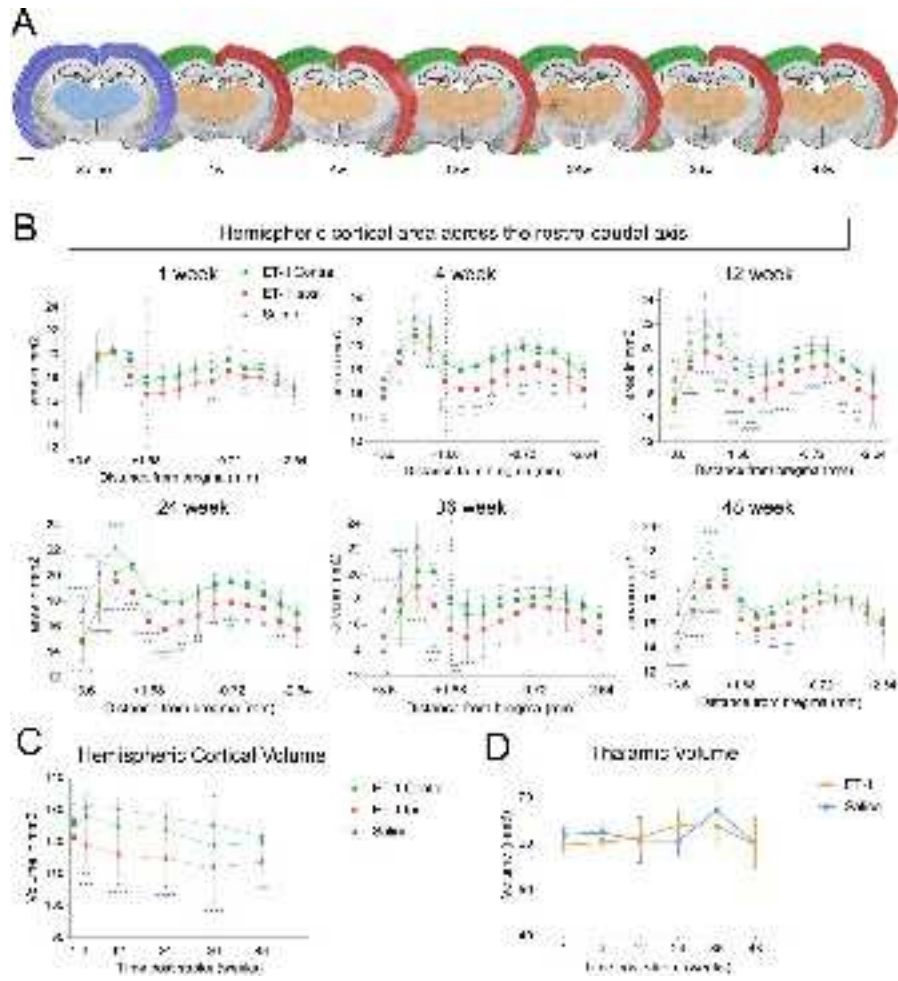
jnr_24939_f1.tif



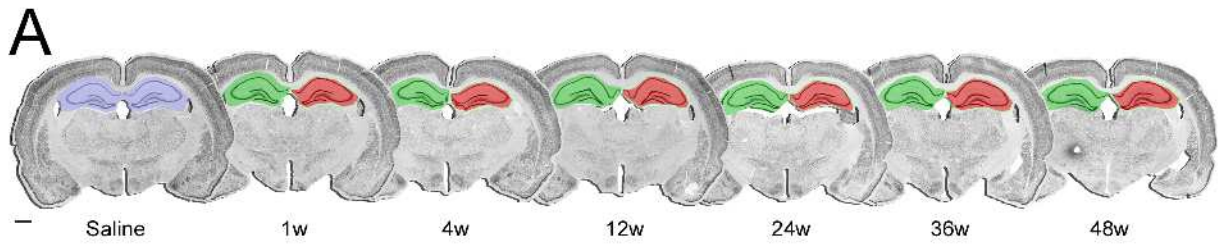
jnr_24939_f2.tif



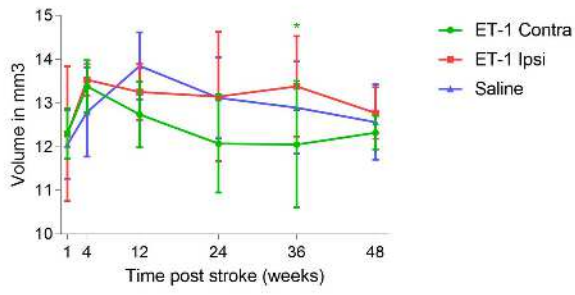
jnr_24939_f3.tif



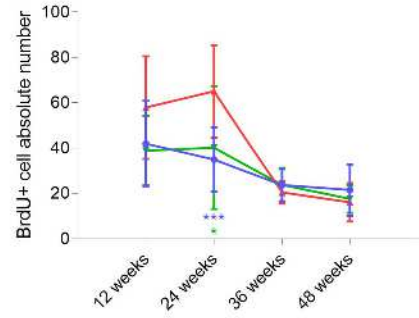
jnr_24939_f4.tif



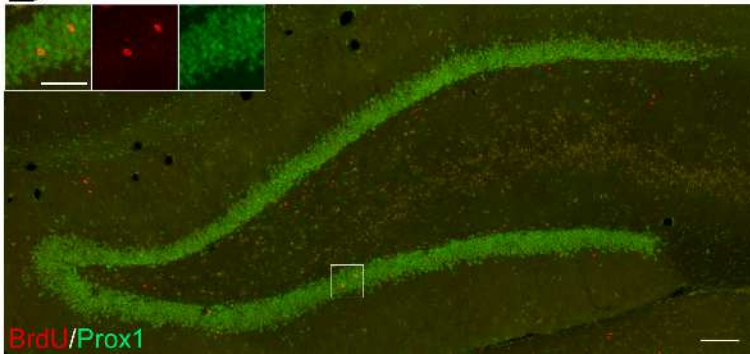
B Hippocampal Volume



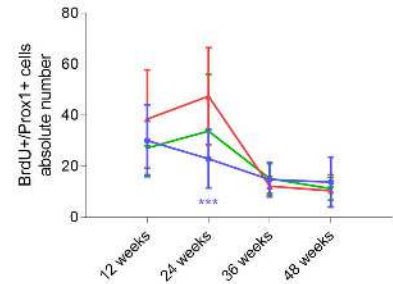
C Number of BrdU+ cells



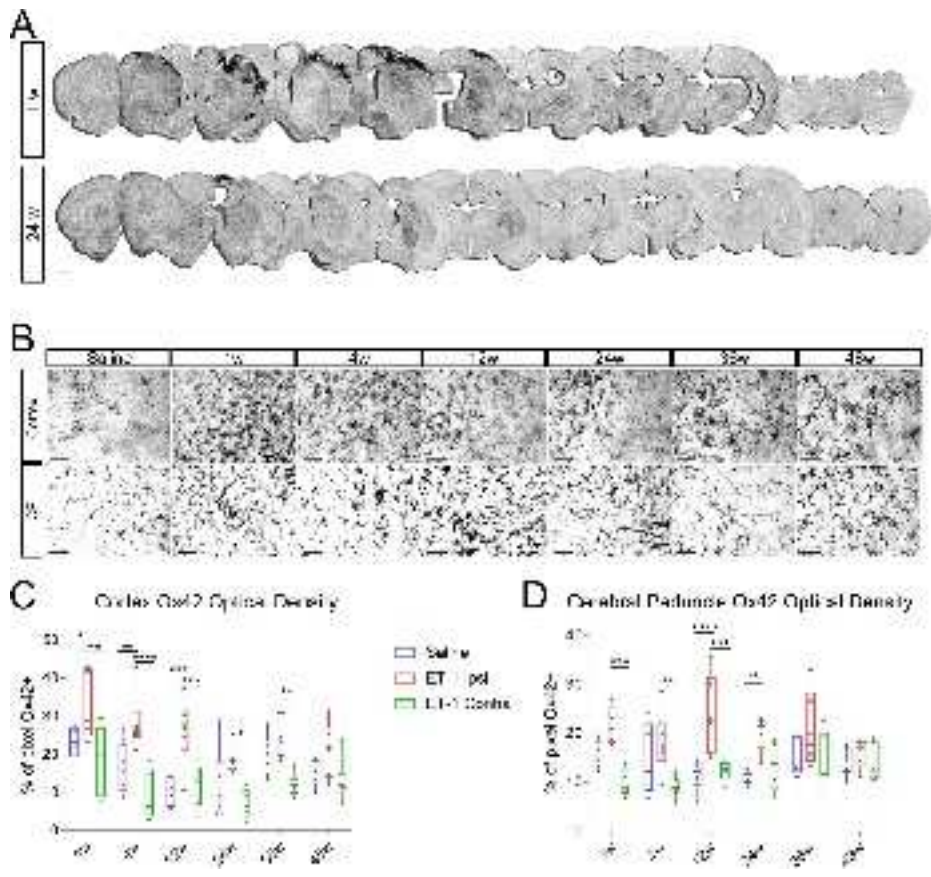
D



E Number of BrdU+/Prox1+ cells



jnr_24939_f5.tif



jnr_24939_f6.tif